Solidification path calculations of Al-Zn-Mg alloys in Al-rich corner

*** Guang-wei Zhao [1, 2], Chong Ding[2], Xin-sheng Gu [3], Xi-Cong Ye [2], Cai-hua Huang [2], and Ming-chun Gu [4]**

1. Hubei Key Laboratory of Hydroelectric Machinery Design & Maintenance, China Three Gorges University, Yichang 443002, China

2. College of Mechanical and Power Engineering, China Three Gorges University, Yichang 443002, China

3. Luoyang Sunrui Titanium Precision Casting Co., Ltd, Luoyang 471000, China

4. Medical College, China Three Gorges University, Yichang 443002, China

Abstract: The solidification paths of Al-Zn-Mg alloys in the Al-rich corner were investigated. The thermodynamic data for the calculation are obtained by direct coupling with the CALPHAD software Thermo-Calc via its TQ6-interface and the COST2 database. The influences of the initial compositions and the extent of solid back diffusion on the solidification path were numerically investigated by sample calculation of the ternary Al-Zn-Mg alloys. The calculation results of solidification paths of the selected alloys: Al-5Zn-3Mg (in wt.%), Al-5Zn-10Mg, Al-2.5Zn-15Mg, Al-10Zn-20.5Mg, Al-8Zn-25Mg, were: L→(L+α-Al), L→(L+α-Al)→(L+α-Al+TAU), L→(L+α-Al)→(L+α-Al+AlMg_β), L→(L+α-Al)→(L+α-Al+TAU)→(L+α-Al+TAU+AlMg_β), L→(L+α-Al)→(L+α-Al+AlMg_β)→(L+α-Al+TAU+AlMg_β), respectively. The results show that the initial compositions and the extent of solid back diffusion have a great influence on solidification path, and the amounts of eutectic phase increase with the decrease of the solid back diffusion coefficient. The equilibrium solute partition coefficients for Zn and Mg in alloys are also calculated and their influence on micro-segregation in the primary solidification of Al-5Zn-10Mg alloy is analyzed.

Key words: solidification path; Al-Zn-Mg alloy; thermo-Calc

CLC numbers: TP391.99 **Document code:** A **Article ID:** 1672-6421(2017)05-443-06

Due to the light weight, good process ability, mechanical properties and weldability, Al-Zn-Mg alloys are extensively used in automobile and mechanical manufacturing, aircraft industry and other high-strength applications. The ternary Al-Zn-Mg system was studied extensively in the past, and most of these studies were focused on the precipitation of microstructure [1-3], phase stability [4, 5], solute distribution [6], and the development of light and high strength alloys [1, 3, 6, 7]. There were also some simulation or calculation studies on this alloy system about diffusion mobility and coefficient [8, 9], prediction of solute distribution [10], and thermodynamics optimization [11, 12]. Due to the lack or unavailability of the corresponding multi-component phase-diagrams/thermodynamic data, the study on solidification path calculation of Al-Zn-Mg alloy was very limited. The approach currently used for the development of these aluminum alloys is the trial-and-error method, which requires great experimental effort to characterize the mechanical behavior of the investigated alloy [7]. Therefore, accurate prediction of the solidification path of a multi-component alloy and the amounts of the secondary phases presented under a given solidification condition is urgently needed for understanding the solidification process and analyzing the microstructure, optimizing the composition and controlling the performances of the solidified alloy, and then improving the efficiency for developing new alloys.

The CALPHAD (CALculation of PHAse Diagram) method has become a powerful tool for solidification simulation. It can calculate multi-component phase equilibrium, liquid and solid surface temperatures, and partition coefficient which are needed in the solidification simulation process of multi-component alloys. Using this method, the computational investigation, especially in prediction of the solidification paths and micro-segregation behavior for multi-component aluminum alloys has been carried out widely in Al-Si-Mg, Al-Cu-

***Guang-wei Zhao**

Male, born in 1981, Ph.D, Associate Professor. Research interests: simulation of solidification transport phenomenon and calculation of solidification path of multi-component alloys.

E-mail: 93757675@qq.com

Received: 2017-07-11; Accepted: 2017-09-10

Mg, Al-Cu-Si and Al-Cu-Zn alloys [13-18]. But the solidification path calculation studies of Al-Zn-Mg alloys were relatively few. Zhao [19] et al. calculated the solidification path of Al-5.3Mg-5.3Zn using the Scheil model and found that the cutoff limit of the residual liquid amount and the simulation temperature step size could have significant impacts on the simulation results. However, as the solid back diffusion of solute is neglected by the Scheil model, the calculation will result in some errors. The solid back diffusion should be considered in the calculation of solidification path [13-18]. Therefore, calculating the solidification path of Al-Zn-Mg alloys with consideration of solid back diffusion and analysing the influences of this parameter on the calculation results, and finding the change rule of the partition coefficient are all worthy to be investigated.

The aims of the present work are to calculate the solidification paths of Al-Zn-Mg alloys using the previously proposed multi-length scale model for ternary eutectic alloys [15]. The model can take into account of any extent of solid back diffusion effects on the solidification path of an alloy. A commercial Thermo-Calc software package/database is linked to the algorithms via its TQ6-interface for instantaneous determination of the related thermodynamic data of the Al-Zn-Mg alloys. The solidification paths of a series of Al-Zn-Mg alloys with different initial compositions in the Al-rich corner, the temperature vs solidification fraction curves, the solidification path and the micro-segregation behavior with different extents of solid back diffusion, and the partition coefficient of Zn and Mg will be calculated and analyzed.

1 Multi-component micro-segregation model

In our previous study [15], a multicomponent/multiphase model for predicting the micro-segregation of ternary alloys was proposed. This model introduced an unified microscale parameter Φ taking a general function form to account for all the possible influential factors, including the partition coefficient, solid fraction, solid diffusion coefficient, dendrite geometrical morphologies and solidification rate, etc. In the present study, this model is used for calculating the solidification path of Al-Zn-Mg alloys. The model can be expressed by Eq.(1)–(3) which describe the three solidification stages of ternary eutectic alloys: primary solidification, binary eutectic solidification and ternary eutectic solidification. More details of this model and the explanation of relative parameters for calculating the solidification paths of ternary eutectic alloys can be seen in Ref. [15]. The algorithms are closely coupled with Thermo-Calc and developed for Al-Zn-Mg alloy system to calculate thermodynamic data needed in the computations.

In the stage of the primary solidification, e.g. α-Al ($0 \le f_S^{i+1} \le f^*_{S(\alpha/2E)}$), the model can be expressed as follows:

$$C_{nL}^{i+1} = \frac{[(f_L\rho_L)^i + \Phi_n^i f_s^i (\rho_s^* k_n)^i]C_{nL}^i}{(f_L\rho_L)^{i+1} + (\Delta f_s^{i+1} + \Phi_n^i f_s^i)(\rho_s^* k_n)^{i+1}} \quad (n=1,2) \tag{1}$$

For a binary eutectic (α+β) solidification ($f^*_{S(\alpha/2E)} \le f_S^{i+1} \le f^*_{S(2E/3E)}$), 2E/3E means transition from (α+β) eutectic to (α+β+γ) eutectic solidification:

$$C_{nL}^{i+1} = \frac{\{(f_L\rho_L)^i + [\Phi^*_{n(\alpha/2E)} f^*_{S(\alpha/2E)} + \Phi^i_{n(2E)}(f_S^i - f^*_{S(\alpha/2E)})](\rho_S^* k_n^{2E})^i\}C_{nL}^i}{\rho_L^{i+1}(1-f_S^i-\Delta f_{S(2E)}^{i+1}) + \{\Delta f_{S(2E)}^{i+1} + [\Phi^*_{n(\alpha/2E)} f^*_{S(\alpha/2E)} + \Phi^i_{n(2E)}(f_S^i - f^*_{S(\alpha/2E)})]\}(\rho_S^* k_n^{2E})^{i+1}} \quad (n=1,2) \tag{2}$$

where

2E — (α+β) eutectic;

3E — (α+β+γ) eutectic;

α/2E— Transition from α-phase to (α+β) eutectic solidification;

k_n — Partition coefficient of the nth component;

i —The ith computational step.

Note that for a binary eutectic solidification in a ternary system, only one of the concentrations, C_{1L}^{i+1} or C_{2L}^{i+1}, is independent; because there exists a (α+β) eutectic trough function in the ternary phase-diagram space for the binary eutectic reaction, $T_{liq(\alpha+\beta)} = T_{liq(\alpha+\beta)}(C_{1L}, C_{2L})$, where subscript liq means liquidus.

In the process of the ternary eutectic (α+β+γ) solidification ($f^*_{S(2E/3E)} \le f_S^{i+1} \le 1.0$), the liquid concentrations for both the solutes 1 and 2 have to keep constant according to Gibbs phase rule:

$$C_{nL}^{i+1} \equiv C_{n(3E)} \quad (n=1,\ 2) \tag{3}$$

In Eqs. (1)–(3), the $f^*_{S(\alpha/2E)}$ and $f^*_{S(2E/3E)}$ are the critical solid-fractions during the solidification transitions of $f_{S(\alpha)} \rightarrow f_{S(2E)}$ and $f_{S(2E)} \rightarrow f_{S(3E)}$, respectively.

It should be mentioned that the unified SBD-parameters Φ_n for the nth solute in Eqs. (1) and (2), can be expressed as:

$$\Phi_n = \theta_n \cdot \varphi_n / (1 + \theta_n \cdot \varphi_n) \quad (n=1,2) \tag{4}$$

where φ_n is a Fourier diffusion number with geometric modification for the (n)th component, θ_n is a non-dimensional parameter for the sensibility of the inter-dendritic liquid concentration variation of the (n)th component to SBD. The non-dimensional parameters of φ_n and θ_n can be written accordingly as:

$$\varphi_n = (D_{nS}/R_f)\boldsymbol{\zeta} \cdot \boldsymbol{A}_{2N} \quad (n=1,2) \tag{5}$$

$$\theta_n = [(1+\beta)k_n f_S]/f_L^2 \quad (n=1,2) \tag{6}$$

where D_{ns} is diffusion coefficient for the (n)th component, R_f is solidification rate, and β is the solidification shrinkage coefficient. The A_{2N} represents a basic geometry-unit vector and Φ_n is a normalized weighting vector corresponding to the basic geometry-unit A_{2N} [15, 18]. According to the present model, Φ_n is a unified parameter reflecting any SBD-effects for the (n)th component. This parameter Φ_n takes a value in the range of [0, 1], where Φ_n=0 and Φ_n=1 represent the two extreme cases of

zero SBD (Scheil model condition) and infinite SBD (Lever-rule conditions), respectively.

2 Calculation results and discussion

2.1 Solidification path calculations with different initial compositions

There are six possible types of solidification path combinations that may occur in a ternary eutectic solidification system with three solid phases A, B and C, i.e. (1) L→(L+A), (2) L→(L+A)→(L+A+B), (3) L→(L+A) →(L+A+C), (4) L→(L+A) →(L+A+B)→(L+A+B+C), (5) L→(L+A) →(L+A+C) →(L+A+B+C), (6) L→(L+A)→(L+A+B+C). In this work, five typcial Al-Zn-Mg alloys were selected to be calculated and listed in Table 1, which can include five possible types of solidification path combinations except the last special one. The calculation parameters of averaged cooling rate and second dendrite arm spacing are 0.454 °C•s^{-1} and 63.28 μm which referred to sand mold solidification experiment results in Ref. [15]. The data/functions used for the other related properties of the investigated ternary aluminum alloy systems in this study are listed in Table 2.

Table 1: Compositions of Al-Zn-Mg alloys used for solidification calculation

Alloys	A	B	C	D	E
Zn (wt.%)	2.5	5	5	8	10
Mg (wt.%)	15	3	10	25	20.5

Table 2: Physical properties for Al-Zn-Mg alloys used in the present calculations

Parameters	Expressions and values	References
Solid diffusion coefficient of Zn in α-Al	$D_{Zn}^{\alpha} = 1.19\times10^{-5}\exp(116.1/(8.314\bullet T))$ [m^2·s^{-1}]	[9]
Solid diffusion coefficient of Mg in α-Al	$D_{Mg}^{\alpha} = 149\times10^{-5}\exp(120.5/(8.314\bullet T))$ [m^2·s^{-1}]	[9]
Density of α-Al	$\rho_{\alpha} = 2.7\times10^{3}$ [kg·m^{-3}]	[16, 18]
Density of TAU ($Al_2Mg_3Zn_3$)	$\rho_{TAU} = 2.69\times10^{3}$ [kg·m^{-3}]	[16, 18]
Density of AlMg_β (Al_3Mg_2)	$\rho_{AlMg\_\beta} = 2.23\times10^{3}$ [kg·m^{-3}]	[16, 18]
Solidification shrinkage of α-phase	β_{α}= 0.043	[18]

Figures 1 and 2 show a comparison for the calculated solidification paths and the temperature *vs* solid fraction (T–f_s) curves of the five Al-Zn-Mg alloys of A, B, C, D and E with different initial compositions. The solidification path of Alloys A (Al-2.5Zn-15Mg) meets the binary trough of (L+α-A1+AlMg_β) at the temperature of 449.88 °C and ends with binary eutectic solidification. Therefore, the solidification path of Alloy A is L→(L+α-Al)→(L+α-Al+AlMg_β) and the volume fractions of primary phase (α-A1) and binary eutectic (α-Al+TAU) are 73.93% and 26.07%, respectively. The calculation results show that Alloy B (Al-5Zn-3Mg) solidifies with 100% primary phase α-Al and experiences the temperature drops from 636.78 °C to 580.04 °C. Therefore, the solidification path of Alloy A is L→(L+α-Al). For Alloy D (Al-8Zn-25Mg), the solidification path meets the binary trough (L+α-Al+AlMg_β) at 448.53 °C and reaches the ternary eutectic point of (L+α-A1+AlMg_β+TAU) at 447.09 °C in the end of the solidification. Therefore, the solidification path of Alloys D is L→(L+α-Al)→(L+α-Al+AlMg_β)→(L+α-A1+AlMg_β+TAU). The volume fractions of the primary phase, binary eutectic, and ternary eutectic of Alloy D are 27.78%, 42.26%, and 29.96%, respectively. It can be seen that the solidification paths of Alloys C (Al-5Zn-10Mg) and E (Al-10Zn-20.5Mg) run down the liquidus surface from the liquidus temperature of 599.81 °C and 524.63 °C and meet the binary trough of (L+α-Al+TAU) at 456.27 °C and 451.14 °C, respectively. The solidification path of Alloy C ends with binary eutectic solidification at 449.14 °C and the volume fraction of binary eutectic is 17.62%. Therefore, the solidification path of alloy C is L→(L+α-Al)→(L+α-Al+TAU). The solidification path of Alloy E reaches the ternary eutectic point at 447.09 °C. Therefore, the solidification path of Alloy E is L→(L+α-Al)→(L+α-Al+TAU) →(L+α-Al+TAU+AlMg_β). The volume fractions of the primary phase (α-A1), binary eutectic (α-Al+TAU), and ternary eutectic (α-A1+AlMg_β+TAU) of Alloy E are 40.97%, 19.33%, and 39.70%, respectively. Above all, it can be found from the calculation results that the initial compositions have a significant effect on the solidification path. The compositions far away from ternary eutectic point such as Alloy B tend to solidify with the primary phase, and the composition near to the binary trough or ternary eutectic point tends to solidify with binary or even ternary eutectic. It also should be noted that the types of the binary eutectic can be different with different initial compositions. The solidification paths of the five selected alloy compositions include the first five possible types of solidification path combinations except the last special one mentioned above in the beginning of this section. In addition, the liquid surface temperatures of the five selected alloys from high to low are 636.78 °C, 599.81 °C, 575.79 °C, 524.63 °C, 496.84 °C of Alloys B, C, A, E, D, respectively. As the types and the amount of the solidified phases can be known from calculation results, solidification path calculation is a useful tool for new alloy development and microstructure analysis.

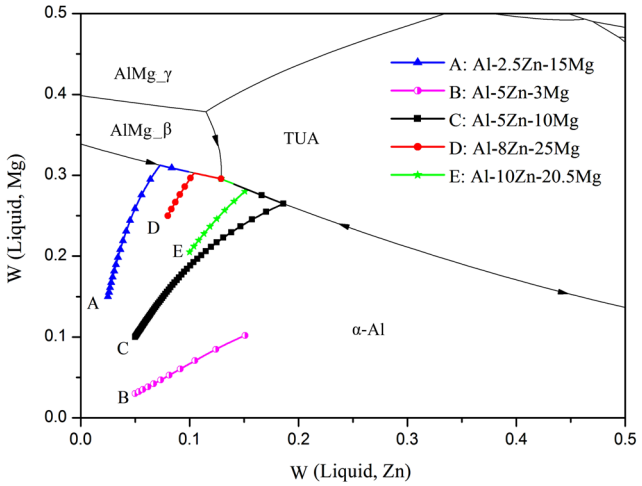

Fig. 1: Calculated solidification paths of Al-Zn-Mg Alloys of A, B, C, D, E

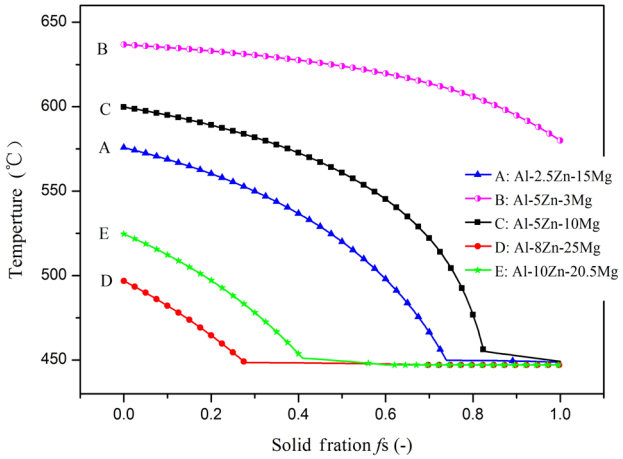

Fig. 2: Calculated temperature *vs* solid fraction (T–f_s) curves of Alloys A, B, C, D, E

2.2 Solidification path calculations with different solid back diffusion parameters

Researchers have shown that the solid back diffusion effects can influence micro-scale solute redistribution behaviors in alloy solidification processes [13-18]. However, few modeling investigations were made on the influences of the solid back diffusion on the solidification path of Al-Zn-Mg alloys. The parameter Φ_n in Eq. (1) and (2) represents the extent of the solid back diffusion effect, which can significantly influence the calculation results of the solidification path [8, 15, 16, 19]. In this section, the solidification path of an Al-Zn-Mg alloy will be calculated to investigate the influence of solid back diffusion on the solidification calculation results. Figures 3 and 4 show the calculated solidification paths and the temperature *vs* solid fraction (T–f_s) curves of alloy Al-5Zn-10Mg of four assumed conditions with different values of parameter Φ_n. It can be seen that the extent of solid back diffusion has an obvious influence on the solidification path calculation results, especially in the primary solidification stage. It can be seen from Fig. 3 that the solidification paths of Al-5Zn-10Mg alloy calculated under conditions of the lever-rule conditions: $\Phi_{Mg}=\Phi_{Zn}=1$, $\Phi_{Mg}=\Phi_{Zn}=2/3$, and $\Phi_{Mg}=\Phi_{Zn}=1/3$ are L→(L+α-Al)→(L+α-Al+TAU), but the final compositions and the amount of phases formed are different due to the different extents of the solid back diffusion effect. The solidification paths reach the binary trough of (L+α-Al+TAU) at 459.15 °C, 458.05 °C, 456.71 °C, and the volume fraction of primary phase is 95.23%, 89.70%, 84.50%, corresponding to the above three assumed conditions of $\Phi_{Mg}=\Phi_{Zn}=1$, $\Phi_{Mg}=\Phi_{Zn}=2/3$, and $\Phi_{Mg}=\Phi_{Zn}=1/3$, respectively. For the conditions of Scheil model ($\Phi_{Mg}=\Phi_{Zn}=0$), the solidification path is L→(L+α-Al)→(L+α-Al+TAU)→(L+α-A1+TAU+AlMg_β), which reaches the binary trough of (L+α-Al+TAU) at 455.12 °C and the ternary eutectic point at 447.09 °C, with 79.54%, 11.93 % and 8.53% of the volume fraction formed as primary phase, binary eutectic and ternary eutectic, respectively. It can be seen that the influence of solid back diffusion on the solidification path is obvious and all the calculation results of the assumed conditions are between the limit conditions of the lever-rule and the Scheil model. The higher the parameter Φ_n, the closer the calculated solidification is to the lever-rule, in which the solid back diffusion is infinite. Figure 5 shows the calculated solid concentrations of Zn

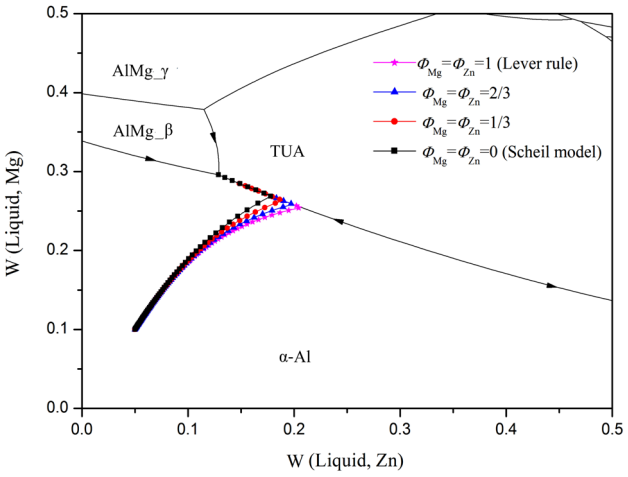

Fig. 3: Solidification paths of Al-5Zn-10Mg alloy with different solid back diffusion parameters Φ_n

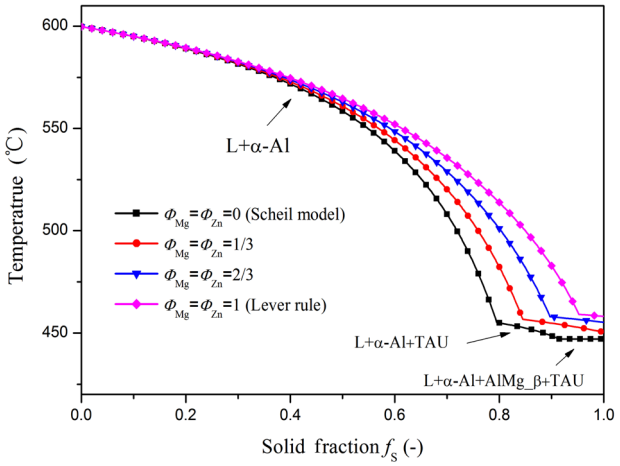

Fig. 4: Calculated temperature *vs* solid fraction (T–f_S) curves of Al-5Zn-10Mg alloy with different solid back diffusion parameters Φ_n

and Mg of the Al-5Zn-10Mg alloys with different solid back diffusion parameters Φ_n. It can be seen that positive segregation is formed in the primary solidification both for the solute Zn and Mg. It is also found that a strong solid back diffusion effect tends to decrease the extent of the micro-segregation.

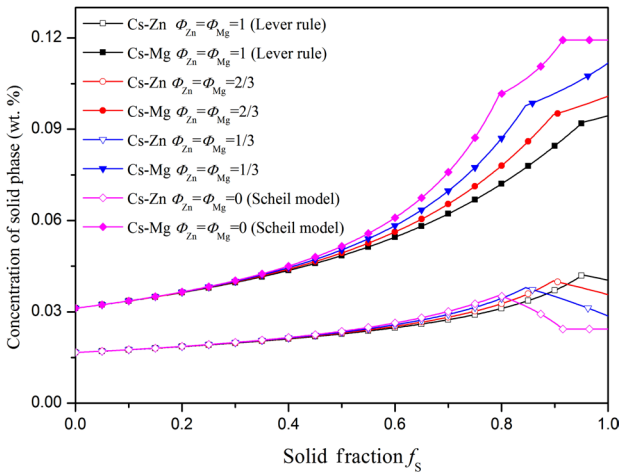

Fig. 5: Calculated solid concentrations of Zn and Mg in Al-5Zn-10Mg alloy with different solid back diffusion parameters Φ_n

2.3 Analysis of partition coefficient

Figures 6 and 7 show the calculation result of the solute partition coefficients, k_{Zn} and k_{Mg}, of Zn and Mg in Alloys A, B, C, D, E using the same parameters listed in Table 2. It should be mentioned that the solute partition coefficient of the binary eutectic stage is calculated as recombination coefficient [15] and can be expressed as the following:

$$k_i^{2E} = g_\alpha^{2E*} k_i^\alpha + g_\beta^{2E*} k_i^\beta \quad (7)$$

where, g_α^{2E*}, g_β^{2E*} are weight fraction of α and β in binary eutectic at the interface of the solid and liquid, k_i^α, k_i^β, k_i^{2E} partition coefficient of solute i in phases α, β and binary eutectic.

It can be seen from Figs. 6 and 7 that k_{Zn} and k_{Mg} are not consistent, but changing continuously in the solidification process. For Alloy B, as solidification proceeds, k_{Zn} and k_{Mg} decrease from 0.3919 to 0.3311 and 0.3096 to 0.2941, respectively. For Alloy A, k_{Zn} decreases from 0.2984 to 0.1888 in the primary solidification and increases from 0.1887 to 0.1892 in the binary eutectic solidification; k_{Mg} increases from 0.3270 to 0.4214 in the primary solidification and decreases from 0.4214 to 0.4129 in the binary eutectic solidification. For Alloy D, k_{Zn} decreases from 0.2277 to 0.1892 in the primary solidification and increases from 0.1892 to 0.1893 in the binary eutectic solidification; k_{Mg} increases from 0.3680 to 0.4112 in the primary solidification and decreases from 0.4112 to 0.4035 in the binary eutectic solidification. At the last stage of ternary solidification, as the liquid and solid concentrations remain unchanged, the partition coefficients are constants of 0.1893 and 0.4035 for Zn and Mg, respectively. For Alloy C, k_{Zn} decreases from 0.3336 to

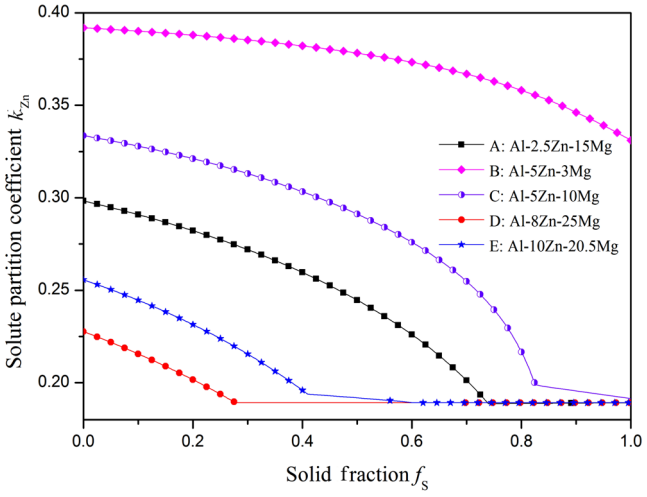

Fig. 6: Calculated solute partition coefficient k_{Zn} of Zn in Alloys A, B, C, D, E

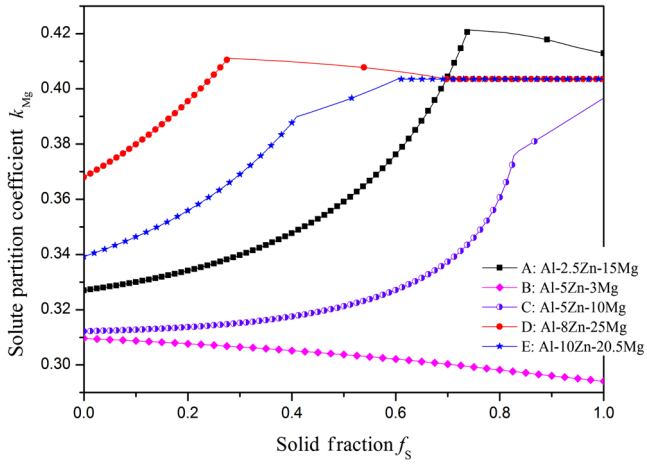

Fig. 7: Calculated solute partition coefficient k_{Mg} of Mg in Alloys A, B, C, D, E

0.2001 in the primary solidification and decreases from 0.2001 to 0.1915 in the binary eutectic solidification; k_{Mg} increases from 0.3122 to 0.3724 in the primary solidification and increases from 0.3724 to 0.3967 in the binary eutectic solidification. For Alloy E, k_{Zn} decreases from 0.2557 to 0.1938 in the primary solidification and decreases from 0.1938 to 0.1893 in the binary eutectic solidification; k_{Mg} increases from 0.3393 to 0.3899 in the primary solidification and increases from 0.3899 to 0.4035 in the binary eutectic solidification. At the last stage of ternary solidification, the same as Alloy D, k_{Zn} and k_{Mg} of Alloy E are constant of 0.1893 and 0.4035 for Zn and Mg, respectively. From the above calculation results, it can be seen that k_{Zn} and k_{Mg} of the Al-Zn-Mg alloy are all less than 1. For the alloys that can reach the binary trough, the change rule of solute partition coefficients in the primary solidification is the same: k_{Zn} decreases and k_{Mg} increases with the solidification process. But for Alloy B that doesn't reach the binary trough, the solute partition coefficient of Mg decreases with the solidification process, which is considered to be related to the slope of the liquid surface. In addition, it could be found from the calculation results of Fig. 5 that the extent of positive micro-segregation of solute Mg is

much more severe than that of Zn. One of the reasons is that k_{Zn} decreases and k_{Mg} increases with the solidification process, as can be seen in Figs. 6 and 7.

4 Conclusions

Based on a previously proposed micro-segregation model [15] by our research team, the solidification paths of Al-Zn-Mg alloys were calculated and the thermodynamic data needed in the calculation were obtained by direct coupling with Thermo-Calc. Through sample calculations, the following conclusions can be made:

(1) The initial compositions have a significant effect on the calculation results of the solidification path. The solidification paths of Alloys A: Al-2.5Zn-15Mg, B: Al-5Zn-3Mg, C: Al-5Zn-10Mg, D: Al-8Zn-25Mg and E: Al-10Zn-20.5Mg are L→(L+α-Al)→(L+α-Al+AlMg_β), L→(L+α-Al), L→(L+α-Al)→(L+α-Al+TAU), L→(L+α-Al)→(L+α-Al+AlMg_β)→(L+α-Al+AlMg_β+TAU), and L→(L+α-Al)→ (L+α-Al+TAU)→(L+α-Al+TAU+AlMg_β), respectively.

(2) The influence of the extent of solid back diffusion on the solidification path is obvious and all the calculation results of the assumed conditions are between the limit conditions of the lever-rule and the Scheil model. The higher the parameter Φ_n, the closer the calculated solidification is to the lever-rule, in which the solid back diffusion is infinite. Positive segregation is formed in the primary solidification of Al-5Zn-10Mg alloy both for the solute Zn and Mg, and a strong solid back diffusion effect tends to decrease the extents of the micro-segregation. The extent of the positive micro-segregation of solute Mg is more severe than that of Zn, because k_{Zn} decreases and k_{Mg} increases with the solidification process.

(3) The calculation results of partition coefficient of the five selected alloys show that both k_{Zn} and k_{Mg} are less than 1, and change continuously with the solidification process. For the alloy that can reach the binary trough, the change rule of solute partition coefficient in the primary solidification is the same: k_{Zn} decreases and k_{Mg} increases with the solidification process. But for the alloy that doesn't reach the binary trough, the solute partition is considered to be related to the slope of the liquid surface. At the ternary eutectic solidification stage, the partition coefficients of Zn and Mg are constant of 0.1893 and 0.4035 for k_{Zn} and k_{Mg}, respectively.

References

[1] Deschampsa A, Texie G, Ringeval S, et al. Influence of cooling rate on the precipitation microstructure in a medium strength Al-Zn-Mg alloy. Mater. Sci. Eng. A, 2009, 501: 133–139.
[2] Deschampsa A, Ringeval S, Texier G, et al. Quantitative characterization of the microstructure of an electron-beam welded medium strength Al-Zn-Mg alloy. Mater. Sci. Eng. A, 2009, 517: 361–368.
[3] Xu K Y, Wang H B, Lu L Y, et al. Study of as-cast microstructure of Al-4.3Zn-1.4Mg alloy. Nonferrous Metals Processing, 2015, 44(3):17–20. (In Chinese)
[4] Rico B, Guido K, Ulrich B, et al. Crystal structure and phase stability of the Φ phase in the Al-Mg-Zn system. Intermetallics, 2013(32): 259–273.
[5] Peter L, Tomasz W, Erwin P K, et al. Thermo-kinetic prediction of metastable and stable phase precipitation in Al-Zn-Mg series aluminium alloys during non-isothermal DSC analysis. J Alloy Compd., 2014, 609: 129–136.
[6] Ramirez-ledesma A L, Chavez C J, Alvarez G O, et al. Effect of growth rate on microstructure and solute distribution of Al-Zn-Mg alloy. Trans. Nonferrous Met. Soc. China, 2015, 25: 1391–1398.
[7] Alexopoulos N D, Pantelakis S G. Evaluation of the effects of variations in chemical composition on the quality of Al-Si-Mg, Al-Cu, and Al-Zn-Mg cast aluminum alloys. JMEP, 2003, 12: 196–205.
[8] Yao J J, Cui Y W, Liu H S, et al. Diffusional mobility for fcc phase of Al-Mg-Zn system and its applications. CALPHAD, 2008, 32: 602–607.
[9] Du Y, Chang Y A, Huang B Y, et al. Diffusion coefficients of some solutes in fcc and liquid Al: critical evaluation and correlation. Mater. Sci. Eng. A, 2003, 363: 140–151.
[10] Soto J, Aramburo G, Gonzalez C, et al. Distribution and prediction of solute in Al-Zn-Mg alloys. Mater. Sci. Eng. A, 2005, 408: 303–308.
[11] Liang P, Tarfa. T, Robinson J A, et al. Experimental investigation and thermodynamic calculation of the Al-Mg-Zn system. Thermochimica Acta, 1998, 314: 87–110.
[12] Yuan Y, Pan F S, Li D J, et al. The re-assessment of the Mg-Zn and Fe-Si systems and their incorporation in thermodynamic descriptions of the Al-Mg-Zn and Fe-Si-Zn systems. CALPHAD, 2014, 44: 54–61.
[13] Jie W Q, Zhang R J, and He Z. Thermodynamic description of multi-component multi-phase alloys and its application to the solidification process. Mater. Sci. Eng. A, 2005, 413-414: 497–503.
[14] Du Q, Eskin D G, and Katgerman L. An efficient technique for describing a multi-component open system solidification path. CALPHAD, 2008, 32: 478–484.
[15] Zhao G W, Li X Z, Xu D M, et al. Thermo-Calc based multi-component micro-segregation model and solidification paths calculations. China Foundry, 2012, 3: 269–274.
[16] Doré X, Combeau H, and Rappaz M. Modelling of micro-segregation in ternary alloys: application to the solidification of Al-Mg-Si. Acta Mater., 2000, 48: 3951–3962.
[17] Vušanović I, Šarler B, Krane M M. Microsegregation during the solidification of an Al-Mg-Si alloy in the presence of back diffusion and macrosegregation. Mater. Sci. Eng. A, 2005, 413-414: 217–222.
[18] Zhao Guangwei, Xu Daming, Song Menghua, et al. Thermo-Calc linked computations of solidification paths of ternary alloys using an extended unified micro-segregation model. Acta Metallurgica Sinica, 2009, 45: 956–963. (In Chinese)
[19] Zhao Y Z, Zhao Y H, Li Q, et al. Effects of step size and cut-off limit of residual liquid amount on solidification simulation of Al-Mg-Zn system with Scheil model. Intermetallics, 2009, 17: 491–495.
[20] Zhang Ruijie, Wang Xiaoying, Jie Wanqi. Solute partition behavior and its influences on solidification process of Al-Si-Mg alloys. The Chinese Journal of Nonferrous Metals, 2003, 13(6): 1483–1487. (In Chinese)
[21] Zhong Bin, Jie Wanqi, Liu Yongqin, et al. Numerical simulation on solute partition and solid fraction evolution in solidification of Al-Cu-Mg alloys. Foundry, 2009, 58(8): 813–816. (In Chinese)

This work was financially supported by the National Natural Science Foundation of China (Grant Nos. 51604161 and 51604162), the Opening fund of Hubei Key Laboratory of Hydroelectric Machinery Design & Maintenance (2017KJX12).